
Deeper Insights into ViTs Robustness towards Common Corruptions

Rui Tian^{1,2} Zuxuan Wu¹ Qi Dai² Han Hu² Yu-Gang Jiang¹

¹Shanghai Key Lab of Intelligent Information Processing,
School of Computer Science, Fudan University

²Microsoft Research Asia

Abstract

Recent literature have shown design strategies from Convolutional Neural Networks (CNNs) benefit Vision Transformers (ViTs) in various vision tasks. However, it remains unclear how these design choices impact on robustness when transferred to ViTs. In this paper, we make the first attempt to investigate how CNN-like architectural designs and CNN-based data augmentation strategies impact on ViTs' robustness towards common corruptions through an extensive and rigorous benchmarking. We demonstrate that overlapping patch embedding and convolutional Feed-Forward Network (FFN) boost performance on robustness. Furthermore, adversarial noise training is powerful on ViTs while Fourier-domain augmentation fails. Moreover, we introduce a novel conditional method enabling input-varied augmentations from two angles: (1) Generating dynamic augmentation parameters conditioned on input images. It conduces to state-of-the-art performance on robustness through conditional convolutions; (2) Selecting most suitable augmentation strategy by an extra predictor helps to achieve the best trade-off between clean accuracy and robustness.

1 Introduction

With the overwhelming advances of Vision Transformers (ViTs) [11, 25], there have emerged numerous ViT-fashion models varying in architecture [4, 14, 55]. As a result, design choices borrowed from classical Convolutional Neural Networks (CNNs) have been incorporated into ViTs to boost performance or efficiency [21, 22, 25, 44]. Meanwhile, benchmarks for robustness towards common corruptions has been proposed [17], expanding concerns over robustness from adversarial-centered settings to ones tackling out-of-distribution data.

Whereas previous studies have unveiled ViTs' superiority over CNNs in robustness [1, 27, 32, 33] and how characteristic components of ViTs affect or boost their resistance towards corruptions [2, 29, 33], no light is shed on influence of design choices migrated from CNNs. In this paper, we undertake first exploration by reviewing on popular ViT backbones and unveil underlying influences of CNN-style design strategies on the robustness of ViTs including overlapping patch embeddings and convolutional Feed-Forward Network (FFN).

In recent literature, plentiful effective methods have been proposed to tackle robustness threats on CNNs [16, 19, 31] while it remains a doubt whether they can be transferred to ViTs straightforwardly. To provide a new insight, we testify the feasibility by implanting previous CNN-based augmentations on ViTs. Since Mixup [57], CutMix [56] and AutoAugment [9] have already been ingrained in ViTs' training paradigm, we lay our main emphasis on more complex methods, *i.e.*, adversarial noise training (ANT) [36] and augmentations in the frequency domain [5].

Motivated by success of dynamic networks, we integrate the idea of conditional computation to adversarial augmentations. On one hand, we propose to dynamically generate sample-specific parameters to produce tailored adversarial perturbations. On the other hand, regarding multiple categories of augmentation, we select the most appropriate one conditioned on inputs via a predictor. The novel conditional augmentation manages to elevate ViTs’ performance against common corruptions.

We derive meaningful findings from an extensive study on popular vision transformers. Our contributions can be summarized as:

- We demonstrate that despite CNNs’ shortcomings in robustness, CNN-derived design choices, *i.e.* overlapping patch embeddings and convolutional feed-forward networks can improve resilience towards robustness even on non-hierarchical ViTs.
- ViTs rely on fundamental augmentations (*e.g.* Mixup, CutMix) in training to a great extent. We demonstrate that adversarial noise training also exhibits advantages on ViTs and structural noise serves as a stronger incentive to promote robustness. On the other hand, we show amplitude-phase interpolation fails to produce any gains on ViTs.
- We tailor differentiable perturbations such as noise, spectral filter and diffeomorphism to adversarial operations conditioned on input. We also demonstrate that their upgrade to dynamic parameters will produce consistent improvements in robustness towards common corruptions.
- We introduce a dynamic augmentation selection strategy conditioned on input samples to seek the best trade-off between clean accuracy and robustness.

2 Related Work

Common corruptions and perturbations In the wake of ImageNet-C [17], which benchmarks robustness towards safety-critical real-world corruptions, research has been committed to overcoming models’ vulnerability towards common corruptions [5, 16, 18, 19, 20, 24, 31]. DeepAugment [16] distorts images by perturbing image-to-image networks. MoEx [24] increases stability of models through swapping mean and standard deviation of image latent features. PixMix [20] uses fractals to create images with structural complexity. Augmentations involve automatic learning are also burgeoning [9, 10, 19, 58]. AutoAugment [9] assigns image with best augmentation policy found by searching algorithm. AugMix [19] augments images with stochastic and diverse augmentations controlled by Jensen-Shannon Divergence. TeachAugment [40] introduces a teacher network to optimize the search space of adversarial augmentations.

Robustness of ViTs Recent studies have reported ViTs’ encouraging characteristic of robustness [1, 32, 33], suggesting that the self-attention architectures contribute to their advantages over CNNs on generalization [1] and demystifying that ViTs tend to be less biased to texture [32]. Efforts have also been made to further enhance robustness on ViTs. By improving on Transformer-based components, Robust Vision Transformer (RVT) is designed to boost performance of model robustness and generalization [29]. In [28], authors build robust global feature representations at the cost of using pre-training to generate discrete tokens to combine with continuous pixel tokens, however making the framework less handy. Existing methods also indicate that AdvProp [49] which proves to be beneficial on CNNs with carefully-designed adversarial training, also strengthens ViTs remarkably through refining attack with pyramidal setting [22]. However, the required multi-step attack demands extensive amount of computing resources. Inspired by ViTs’ intrinsic superiority and existent methods, we aims to resort to relatively simple yet strong plug-and-play techniques to boost vision transformers’ robustness to their full potential, as expounded in section 4.

Adversarial augmentation Adversarial training is a widely-acknowledged strategy of defending models from attacks. In general, it executes attack and consequent defense alternately on the basis of a min-max optimization. Motivated by the effectiveness of adversarial training, min-max optimization is tailored to a broader variety of tasks, including coping with common corruptions risks [22, 38, 49]. Mild and much less time-consuming data augmentations can serve as the attack function as well as bring about considerable improvements against common corruptions [38]. Adversarial Noise Training (ANT) [36] plays a beneficial role by adding random Gaussian Noise adjusted by a simple 4-layer convolution trained in adversarial manner. AugMax [42] achieves significant performance rise

Table 1: We evaluate 5 genres of popular ViTs, *i.e.*, DeiT [41], ViT [11], PiT [21], PVT [43, 44] and Swin Transformer [25], among which the last three backbones are hierarchical in design. Bold numbers indicate weak results of some hierarchical genre of ViTs. The listed results are sorted by Parameters in ascending order.

Model	Hierarchical	#Param(M)	IN	IN-C	
			Acc \uparrow	Acc \uparrow	mCE \downarrow
PiT-T [21]	✓	4.85	72.84	45.70	69.11
ViT-T [11]	✗	5.70	75.49	42.64	72.50
DeiT-T [41]	✗	5.70	72.14	44.23	71.13
PVTv1-T [43]	✓	13.2	75.00	37.94	79.56
PVTv2-B1 [44]	✓	14.0	78.70	50.81	62.65
DeiT-S [41]	✗	22.0	79.83	57.20	54.60
ViT-S [11]	✗	22.1	81.40	58.31	52.95
PiT-S [21]	✓	23.5	80.98	58.88	52.47
PVTv1-S [43]	✓	24.5	79.79	47.89	66.89
PVTv2-B2 [44]	✓	25.4	82.02	58.92	52.56
Swin-T [25]	✓	28.3	81.16	51.59	61.96
PVTv1-M [43]	✓	44.2	81.31	51.34	62.39
Swin-S [25]	✓	49.6	83.17	57.16	54.92
PVTv1-L [43]	✓	61.4	81.72	53.33	59.86
PiT-B [21]	✓	73.8	82.39	62.39	48.16
PVTv2-B5 [44]	✓	82.0	83.77	64.12	45.90
DeiT-B [41]	✗	86.6	81.80	62.06	48.52
Swin-B [25]	✓	88.0	83.75	57.51	66.70

by learning a worst-case combination of random augmentations. Adversarial Batch Normalization (AdvBN) [39] withstands corruptions through generating the most difficult perturbations on mean and standard deviation of features. To our knowledge, any differentiable data augmentations can be practiced adversarially. Hence, we take advantage of different adversarial data augmentations in our conditional augmentations for the sake of better results.

Dynamic networks Through adapting parameters and structures to specific input, neural networks are transformed into dynamic states, contributing gains in accuracy [6, 52], efficiency [35, 37] or adaptiveness [61]. According to [13], dynamic networks can be divided into three different categories focusing respectively on input samples, spatial locations and temporal information. Regarding with instance-wise dynamic networks, convolutions with dynamic parameters [6, 52, 59] bring about increase in capacity of representations with high computational efficiency and cope with input better with feeding selected informative features into models [37]. While extensive data augmentation methods have been designed, most existing algorithms are implemented identically for different samples. By virtue of dynamic networks, we propose a novel conditional augmentation strategy from the aspects of both dynamic parameters and input-dependent augmentation category.

3 Insights into Robustness of ViTs

We analyze the robustness of ViTs with regard to CNN-borrowed structural designs and transferability of augmentations devised for CNNs. Among our explorations, positive effects of overlapping patch embedding and convolutional feed-forward network on robustness are uncovered. We also reveal ViTs’ strong reliance on fundamental augmentations and efficacy of adversarial noise training.

3.1 Backbone Design Choice Exploration

To acquire deeper insight into how design choices originated from CNNs affect ViTs robustness towards common corruptions, we evaluate prevailing ViT backbones on ImageNet and ImageNet-C with focus on how hierarchical ViTs behaves. Consequently, we come up with several research questions through analysis and take a closer look at the effects of CNN-derived backbone components.

Table 2: Results of DeiT-S with different feed-forward designs. Method without Conv. equals setting of DeiT-S [41]. DWConv [7] is implemented with 3×3 kernel and stride of 1. We denote Conditional DWConv as Cond DWConv and keep kernel size to 3 with setting N to 32.

Feed-Forward Designs	IN Acc \uparrow	IN-C Acc \uparrow	mCE \downarrow
w/o Conv.	79.83	57.20	54.60
DWConv	79.93	58.91	52.41
Cond DWConv	79.79	58.27	53.27

Table 3: Results of DeiT-S with different patch embedding designs. Method with FC.(Fully-Connected layers) is equivalent to ViT-S [11]. Conv. refers to convolution-based patch embedding and method with Conv. 16×16 is exactly same as DeiT-S [41].

Patch Embedding	IN		IN-C
	Acc \uparrow	Acc \uparrow	mCE \downarrow
FC.	80.37	57.69	53.99
Conv. 16×16	79.83	57.20	54.60
Conv. 18×18	80.45	58.93	52.40
Conv. 20×20	80.40	58.37	53.10
Conv. 24×24	79.77	58.51	52.94

ViT is first introduced with fixed spatial dimensions in all layers [11]. Hierarchical genre of ViTs borrow the classical down-sampling idea from CNNs to shrink spatial size of features progressively [21, 22, 25, 44]. Though models such as PVTv1 [22] and Swin Transformer [25] demonstrate solid performance in clean accuracy on ImageNet, they suffer acute weakness on corrupted data, as we observe from Table 1. However, considering strong robustness PiT [21] and PVTv2 [44] have presented, hierarchical architecture do NOT necessarily contribute to deficiency in robustness. Due to space limitations, we provide further analysis on Swin Transformer in Appendix A.1.

It is also worth-mentioning that growth of PVTv2 in both clean and corrupted domains is remarkable compared to PVTv1. We conduct a further exploration of its architectural improvement, involving (1) *overlapping patch embedding* and (2) *convolutional feed-forward networks*. We wonder whether similar strategies will boost robustness performance of ViTs without pyramidal structures. Therefore, we apply above modifications on DeiT-S [41] respectively.

Overlapping patch embedding In vanilla ViT [11], encoding of an image $x \in \mathbb{R}^{C \times H \times W}$ starts with segmenting it into sequences of patches sized of $p \times p$, where p denotes the required patch size. Flattened patches $x_p \in \mathbb{R}^{T \times (p^2 \times C)}$ are mapped to tokens $t \in \mathbb{R}^{T \times D}$ by a fully-connected layer. Later in DeiT [41], patch embedding is implemented with convolution whose kernel size and stride are p . As a result, pixels within a single patch is operated by identical kernels. In contrast to these non-overlapping patch embeddings, CNNs stem from applying convolutions among overlapping spatial areas.

As adopted by PVTv2, overlapping patch embedding take pieces from CNNs by expanding the scope of convolution to surrounding pixels of a patch, in other words, increasing the kernel size. We leverage the concept of overlapping patch embedding in DeiT. To encode extended area within k pixels around the original patch in each single token, we adopt convolution with $((p+2k) \times (p+2k))$ kernel and additional zero padding while leaving the stride size fixed. Hence, horizon of convolution is enlarged and output dimension is kept unchanged simultaneously.

In practice, with p set to 16, we conduct experiments with k varying in 1, 2 and 4. Results from Table 3 displays a convincing conclusion that *overlapping patch embeddings conduce to robustness*. Specifically, models with overlapping patch embedding present more stability towards perturbations of noise, contrast and JPEG compression (please refer to Appendix B).

Convolutional FFN Researchers have been trying to incorporate convolutions into ViT backbones [47, 54]. Depth-wise convolution (DWConv) [7] is a special form of convolution which applies a single filter to each input channel (input depth). We follow PVTv2 by adding a depth-wise convolution to each feed-forward block in DeiT. For output $f_i^1 = [f_{i,cls}^1, f_i^{1*}]$ of i -th attention layer, with class token $f_{i,cls}^1$ projected identically, the DWConv-affiliated FFN functions are as follows,

$$\begin{aligned} f_i^{2*} &= \text{FC}_i^2(\text{GeLU}(\text{DWConv}_i(\text{FC}_i^1(f_i^{1*})))), \\ f_i^2 &= [f_{i,cls}^1, f_i^{2*}]. \end{aligned} \tag{1}$$

f_i^2 is then fed into the following ViT blocks after residual connection. As Table 2 shows, *convolutional FFN design also invokes growth of robustness*.

While class token hasn't been involved in convolution, motivated by CondConv [52], we introduce Conditional DWConv to generate convolution kernels dynamically according to class tokens. Image tokens $\mathbf{f} \in \mathbb{R}^{(T_h \times T_w) \times D}$ are transformed to shape of $\mathbb{R}^{D \times T_h \times T_w}$ before fed into convolution and class tokens $\mathbf{X} \in \mathbb{R}^{1 \times D}$ are projected to space of \mathbb{R}^N by a fully-connected layer, where N indicates the number of learnable kernels. Consequently, we proceed to obtain a conditional kernel weight $\mathcal{W}(\mathbf{X})$,

$$\begin{aligned}\mathcal{R}(\mathbf{X}) &= \{w_1, w_2, \dots, w_N\}, \\ \mathcal{W}(\mathbf{X}) &= w_1 \cdot K_1 + \dots + w_N \cdot K_N,\end{aligned}\tag{2}$$

where K_i refers to N different kernels sharing same shape with original DWConv and output of network can be acquired by $\text{DWConv}(f, \mathcal{W}(\mathbf{X}))$. However, experiment suggests that adding conditional convolution to DeiT leads to no further gain in robustness (Table 3).

Nevertheless, the results are still better than that without Conv, highlighting the potential contributions of convolutions to robustness.

3.2 Augmentation Methods Exploration

As mentioned in section 2, adversarial augmentations have been widely proven to be effective. Among all existing methods, we lay our emphasis on Adversarial Noise Training (ANT) [36] as it initiates adjusting augmentation parameters by a light neural network. We also pay attention to fourier-based augmentations but fails to find its effectiveness to boost robustness on ViTs.

3.2.1 Adversarial Noise Training

ANT [36] has achieved success in bringing about great advances on robustness towards common corruptions with CNNs. Random noise are first fine-tuned and cast on images to play the most harmful role. To specify, Gaussian (Eq. 3a) Noise and Speckle Noise (Eq. 3b) are generated to perturb image x ,

$$\Sigma_1(x) = x + \text{clip}_p(\sigma_\delta, \epsilon),\tag{3a}$$

$$\Sigma_2(x) = x + \text{clip}_p(\sigma_\delta \cdot x, \epsilon),\tag{3b}$$

among which $\sigma_\delta \in \mathbb{R}^{C \times H \times W}$ obeys the distribution of $\mathcal{N}(\mathbf{0}, \delta^2)$. The clipping function clip_p confines noise within boundary of ϵ for L_p norm. We conduct ANT on ViT (denoted as f_θ) with the following optimization objective:

$$\begin{aligned}\min_{\theta} \max_{\tau} & \mathbb{E}_{(x,y) \sim D} \mathbb{E}_{\sigma_\delta \sim \mathcal{N}(\mathbf{0}, \delta^2)} [\mathcal{L}_{CE}(f_\theta(x + \text{clip}_p(\mathcal{P}_1(\sigma_\delta), \epsilon), y)], \\ \min_{\theta} \max_{\tau} & \mathbb{E}_{(x,y) \sim D} \mathbb{E}_{\sigma_\delta \sim \mathcal{N}(\mathbf{0}, \delta^2)} [\mathcal{L}_{CE}(f_\theta(x + \text{clip}_p(\mathcal{P}_2(\sigma_\delta \cdot x), \epsilon), y)],\end{aligned}\tag{4}$$

where \mathcal{P} denotes noise generators, typically consist of 4-layer convolutions with 1×1 kernels. In inner loop of (Eq. 4), generator is first enhanced to produce most harmful noises, serving as attack in adversarial training; And then ViT optimizes its resistance by learning from noisy input, as the defense phase referred in outer loop.

Adversarial noise training is effective For simplicity, we attack DeiT-S with ANT generator and defend on noisy data once per iteration. During attack, all data should be assigned with noise generated by ANT and 50% of clean data is reserved at defense. Furthermore, we still keep the experience replay setting in ANT, restarting generators with new parameters in each epoch with 20% of samples augmented by randomly-drawn previous noise generators.

Following procedure similar with original ANT, we train on ViTs for 300 epochs, employing AdamW [26] optimizer for classifiers with a cosine decay learning rate scheduler and Adam optimizer for

Table 4: We conduct extensive experiments of adversarial noise training on DeiT, PiT and ViT. Pre-trained filled with \checkmark stands for fine-tuning experiments, *i.e.* models are initialized with weights from official open source while ViT-S is an exception as we train it from-scratch on basis of DeiT’s augmentations and regularizations. Methods start with Cond refer to ones strengthened with our dynamic parameters strategy. We also compare our conditional method on base model with state of the art below. Additional ablation studies are attached in supplementary material.

Method	Pre-trained	Norm	IN	IN-C	IN-C
			Acc \uparrow	Acc \uparrow	mCE \downarrow
DeiT-S [41]	\times	-	79.83	57.20	54.60
+ finetune 300 ep.	\checkmark	-	81.16	59.06	52.24
+ ANT Gaussian 1×1	\times	80	78.91	59.92	51.20
+ ANT Gaussian 1×1	\checkmark	80	80.27	62.51	48.09
+ ANT Gaussian 1×1	\checkmark	130	80.24	62.76	47.81
+ ANT Gaussian 3×3	\checkmark	80	80.52	62.42	48.18
+ ANT Gaussian 16×16	\checkmark	80	80.40	62.30	48.35
+ ANT Speckle 1×1	\checkmark	80	80.35	62.74	47.82
+ ANT Speckle 3×3	\checkmark	80	79.80	61.60	49.25
+ Cond ANT Gaussian 1×1	\checkmark	80	80.18	63.16	47.28
+ Cond ANT Speckle 1×1	\checkmark	80	80.15	63.28	47.18
PiT-S [21]	\times	-	80.98	58.88	52.47
+ Cond ANT Speckle 1×1	\checkmark	80	80.74	63.64	46.63
ViT-S [11]	\times	-	80.37	57.69	53.99
+ Cond ANT Speckle 1×1	\checkmark	80	80.60	64.08	46.18
DeiT-B [41]	\times	-	81.80	62.06	48.52
RVT-B [29]	\times	-	82.60	-	46.80
Discrete ViT [28]	\times	-	79.48	-	46.22
ViT-B + Adv Pyramid [22]	\times	-	81.71	-	44.99
DeiT-B + Cond ANT Speckle 1×1	\checkmark	80	82.19	67.00	42.41
DeiT-B + Cond ANT Speckle 1×1	\checkmark	130	82.35	68.38	40.68
					66.46

noise generators. When training from scratch, we set learning rate for ViTs as $1e^{-3}$ on the basis of a batch size of 1024, and decrease the learning rate to $4e^{-4}$ for fine-tuning tasks. The learning rate of noise generators is fixed to $8e^{-5}$. All augmentation strategies in DeiT training [41] are kept since they turn out to be beneficial to final results (Table 5). We hold on to the same strategy unless mentioned otherwise.

In view of experiment results displayed in Table 4, effectiveness of ANT on ViTs can be validated. In accordance with findings on CNNs, besides noises, ANT gives an impetus to robustness on other corruptions. Also, despite the fact that a trade-off between performance on clean and corrupted data is demonstrated on DeiT-S, DeiT-B benefits in both domains. We owe this result to larger capacity of base ViT models and suggest that heavy augmentations may serve as the catalyst for better performance of large ViTs.

Structural noise is more powerful We build adversarial generators both on Gaussian and Speckle noise. Speckle noise amplified by generators applied on 1×1 pixel region can bear most structural information of original images. As it manifests in Table 4 that experiments with 1×1 speckle-noise achieve best performance on ImageNet-C. However, as a performance drop is witnessed, spatial information might be destructed by convolutions with 3×3 kernels, since more attention has to be paid to local correlation.

Basic augmentations are necessary Since we train ANT on top of DeiT’s paradigm, four basic augmentations, *i.e.*, Mixup [57], CutMix [56], ColorJitter and AutoAugment [9] are involved so as to stabilize the training and boost clean performance. There is a necessity to explore interplay between additive adversarial noise and previously-adopted augmentations. Results in Table 5 indicate that *ViTs are highly dependent on basic perturbations*. Absence of any method gives rise to deficiency on either ImageNet or ImageNet-C.

Furthermore, we argue that sequence of Mixup, CutMix and noise augmentations is also crucial to final results. We make the investigation with 3 different means: (1) We first implement normalization on data, followed up with Mixup or CutMix and noise is added at last; (2) Noise is first applied

Table 5: Ablations on exempting basic augmentation from Gaussian ANT 1x1 training on pre-trained DeiT-S. The baseline includes all augmentations. In each run, we remove one type of augmentation.

Augmentation	IN			IN-C		
	Acc↑	Acc↑	mCE↓	Acc↑	Acc↑	mCE↓
ANT 1x1	80.27	62.51	48.09			
- Mixup	80.65	59.99	51.07			
- CutMix	79.94	62.13	48.62			
- ColorJitter	80.41	62.12	48.53			
- AutoAugment	79.68	58.75	52.89			

Table 6: Ablations on sequence of augmentations in Gaussian ANT 1x1 training on pre-trained DeiT-S, where Mix. is the abbreviation of Mixup and CutMix. In the following, our default experimental setting is same with (3).

Augmentation Sequence	IN			IN-C		
	Acc↑	Acc↑	mCE↓	Acc↑	Acc↑	mCE↓
(1) Early Mix.	80.76	60.45	50.56			
(2) Full Mix.	80.19	61.95	48.66			
(3) Separate Mix.	80.27	62.51	48.09			

followed by normalization and Mixup or CutMix is fulfilled along the whole batch; (3) Noise is first applied followed by normalization while Mixup or CutMix is conducted separately among clean and noisy data. Method (3) is proved to be the optimal in view of results in Table 6.

Training with masks shows no merit Patch-wise augmentation has been adopted in recent works [12, 29] and masked image modeling [15, 50] becomes a new trend on ViTs. To take a closer at characteristics of ViTs, we employ ANT in a masked manner. Instead of training on 50% noisy images, training with masks indicates only imposing adversarial Gaussian noises on randomly masked patches of all images. Unlike previous results, numbers in Table 7 manifest that noisy-masked training on pre-trained models fail to generalize well on corrupted data while descending less in clean performance. The phenomenon is in line with discovery in [32], where ViTs are reported to be robust against occlusions. In essence, ViTs rely little on corrupted patches and succeed to perceive semantic information from the remaining clean patches.

Table 7: Results of masked adversarial noise training on DeiT-S. † indicates training from scratch. All experiments are conducted with noise generated by ANT Gaussian 1x1.

Method	IN			IN-C		
	Acc↑	Acc↑	mCE↓	Acc↑	Acc↑	mCE↓
+ 50% mask †	79.28	57.05	54.81			
+ 30% mask	80.90	59.89	51.41			
+ 50% mask	80.63	59.42	51.99			
+ 70% mask	80.58	59.99	51.26			

Table 8: Results of amplitude interpolation on DeiT-S. † indicates training from scratch and p denotes portion of data augmented with amplitude interpolation.

Method	IN			IN-C		
	Acc↑	Acc↑	mCE↓	Acc↑	Acc↑	mCE↓
DeiT-S	79.83	57.20	54.60			
+ APR $_{p=0.5}^*$	80.16	59.91	51.19			
+ APR $_{p=0.5}^*$ †	74.97	51.67	61.84			

3.2.2 Augmentations in Fourier Domain

According to [53], adversarial augmentations are blind to corruptions in low-frequency domain, *i.e.*, Fog and Contrast. ANT also induces a slight drop in corruption categories of Fog on ViTs. Therefore, We perform an augmentation in frequency domain, which is similar to APR [5], a method effective to fuel robustness towards low-frequency corruptions on CNNs by swapping amplitude components between samples. Besides, impressed by FACT [51], who improves models on domain generalization tasks by linearly interpolating between the amplitude spectrums of two images, we equip APR with interpolation. For samples x and x' chosen randomly within same batch, our method can be denoted as

$$\begin{aligned} \tilde{\mathcal{A}}(x) &= (1 - \lambda)\mathcal{A}(x) + \lambda\mathcal{A}(x'), \\ \mathcal{F}(x) &= \tilde{\mathcal{A}}(x) \cdot e^{-j \cdot \mathcal{P}(x)}, \end{aligned} \tag{5}$$

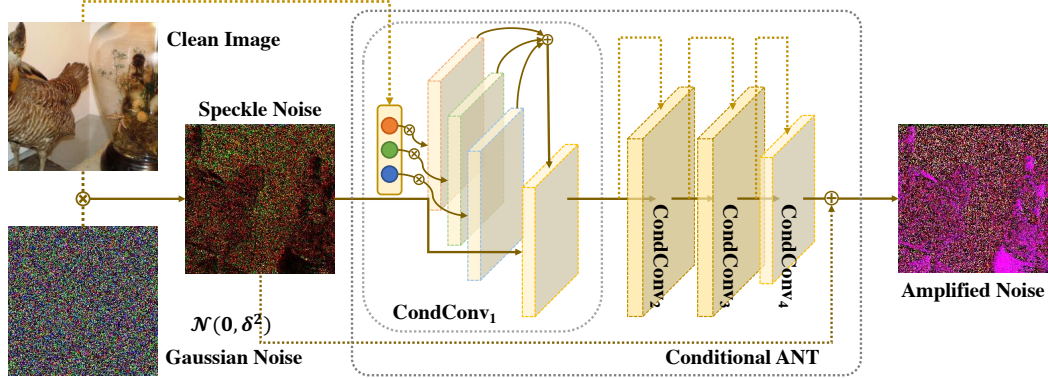


Figure 1: An overview of Conditional ANT framework. Given a clean image and random Gaussian noise, speckle noise is acquired by multiplication. Both clean image and noise will be fed into conditional ANT composed of 4 layers of 1×1 CondConv and a residual connection. Afterwards, to obtain final augmented input, the generated noise with restricted norm will be added to clean image.

where $\mathcal{A}(x)$ denotes the amplitude component of x and $\mathcal{P}(x)$ refers to the phase component, λ is obtained by randomly drawn from $\mathcal{N}(0, 0.5)$.

Amplitude interpolation is bad on ViTs Unlike CNNs, performance on robustness even declines with fourier-based augmentations, as shown in Table 8. We wonder if layered-up augmentations are too difficult to learn and consequently relieve training with Mixup and CutMix. However, it undergoes a failure of stable training. This finding also gives credence to conclusion that ViTs are heavily dependent on basic augmentations.

4 Conditional Adversarial Augmentations

While ANT is an effective augmentation strategy, it produces a noisy image regardless of the visual content of input samples with “one-size-fits-all” parameters. Recently, there is a growing interest in dynamic networks in CNNs that generate sample-specific parameters conditioned on inputs [6, 52, 59]. This motivates us to explore dynamic techniques in adversarial augmentations for improved performance. In this section, we start by introducing input-dependent augmentation on top of dynamic networks. We instantiate conditional computation for augmentations from two different aspects: (1) Dynamically generating augmentation parameters for each input instance; (2) Dynamically choosing the augmentation type for each training sample. We demonstrate our methods in detail as below.

4.1 Conditional ANT

Our goal is to generate sample-specific noise conditioned on input images. In other words, we aim to apply dynamic weights to derive augmentations superior to ANT. To this end, we resort to CondConv [52] which replaces vanilla convolution layers with conditional convolutions in noise generators. Specifically, image x will be mapped to a space of N expert weights by a routing function $\mathcal{R} : \mathbb{R}^{C \times H \times W} \rightarrow \mathbb{R}^N$. Consequently, a customized kernel \mathcal{W} will be generated by the image-specific weights in the same way as conditional DWConv (Eq. 2). At present we stick to the original routing function in CondConv, which can be elaborated as,

$$\mathcal{R}(x) = \text{Sigmoid}(\text{FC}(\text{GlobalAveragePool}(x))). \quad (6)$$

Next, we proceed to fine-tune on ViTs via conditional ANT with $N = 16$. Results in Table 4 suggests that *the dynamic techniques achieves state-of-the-art performance*, which surpasses the best performance of ANT by 0.5% on DeiT-S for the ImageNet-C accuracy. Also, compared to other state-of-the-art method on base model, our results on Deit-B is highly competitive both on ImageNet and ImageNet-C.

Table 9: Results of spectral filter (SF.) on pre-trained DeiT-S.

Method	IN			IN-C		
	Acc↑	Acc↑	mCE↓	Acc↑	Acc↑	mCE↓
+ SF. 3x3	80.92	59.92	51.35			
+ Cond SF.3x3	81.08	60.44	50.60			

Table 10: Results of diffeomorphisms (Diffeo.) on pre-trained DeiT-S.

Method	IN			IN-C		
	Acc↑	Acc↑	mCE↓	Acc↑	Acc↑	mCE↓
+ Diffeo.	81.01	60.91	49.92			
+ Cond Diffeo.	80.74	61.63	49.00			

4.2 Dynamic Parameters

As we demonstrate in section 4.1, speckle noise combined with conditional adversarial training has already brought about considerable improvements in robustness, but it still has disadvantages over certain corruptions (*e.g.* Fog) and is short in clean performance. To explore greater potential of dynamic parameters, we hypothesize that any differentiable perturbations can be adapted to be conditionally produced. To support it, we introduce two other perturbations, which are adopted in [31] and then we verify the increase brought about by our methods.

Spectral perturbations Following [31], we build a random spectral filter Ψ to perturb image x in spectral domain,

$$\Psi(x) = x * (\omega_k + \sigma_{k,\delta}), \quad (7)$$

where $*$ is a convolution operator with kernel shaped in $k \times k$, ω_k represents the according Dirac delta filter, satisfying $x * \omega_k = x$. $\sigma_{k,\delta} \in R^{k \times k}$ is initialized with $\mathcal{N}(\mathbf{0}, \delta^2)$ and can be amplified in latter training. On top of that, we apply the filter separately on RGB channels, which will arise to a shift in color as well.

Spatial perturbations Stability towards diffeomorphism is proven to bear strong correlations with model performance [34]. We precede with the proposed maximum-entropy diffeomorphism Φ to generate spatial perturbations on x coordinated with $u(i, j)$,

$$\begin{aligned} [\Phi x](u) &= x(u - (\phi_i(u), \phi_j(u))), \\ \phi_i &= \sum_{m^2+n^2 \leq c} \sigma_{\rho_{m,n}} \sin(m\pi i) \sin(n\pi j), \end{aligned} \quad (8)$$

where $\sigma_{\rho_{m,n}} \sim \mathcal{N}(\mathbf{0}, \rho_{m,n}^2)$, $\rho_{m,n} = \sqrt{\mathcal{T}/(m^2 + n^2)}$ and then the overall magnitude is confined by \mathcal{T} and c . Diffeomorphism results in displacement of pixel coordination, which would raise difficulty in latter training if the smooth value were pruned to get discrete index. Therefore, we use bi-linear interpolation instead to assure of differential computation.

Learning worst perturbations At the heart of our method, random variables are enforced by simple yet effective conditional convolutions. We adapt the empirical design of conditional ANT 1x1 to manipulating random parameters in augmentation generators \mathcal{P}_τ^1 and \mathcal{P}_τ^2 . Specifically, optimization functions for spectral filter Ψ and diffeomorphism Φ are similar to that for noise,

$$\min_{\theta} \max_{\tau} \mathbb{E}_{(x,y) \sim D} \mathbb{E}_{\sigma \sim \mathcal{N}(\mathbf{0}, 1)} [\mathcal{L}_{CE}(f_\theta(x * (\omega + \mathcal{P}_\tau^1(\sigma, x) \cdot \delta)))], \quad (9a)$$

$$\min_{\theta} \max_{\tau} \mathbb{E}_{(x,y) \sim D} \mathbb{E}_{\sigma \sim \mathcal{N}(\mathbf{0}, 1)} [\mathcal{L}_{CE}(f_\theta(x(u - (\phi(u, \mathcal{P}_\tau^2(\sigma, x) \cdot \rho))))]. \quad (9b)$$

Note that δ , c and \mathcal{T} are manually-set hyper-parameters to moderate augmentation tensity. Specifically, we take $\delta = 0.2$, $c = 20$, $\mathcal{T} = 1e^{-4}$ for implementation. The training procedure for attack and defense is identical with one stated in section 3.2.1.

Dynamic parameters can boost robustness Our methods strength augmented data distribution through differentiable and input-variant operations. Results in Table 9 and Table 10 witness improve-

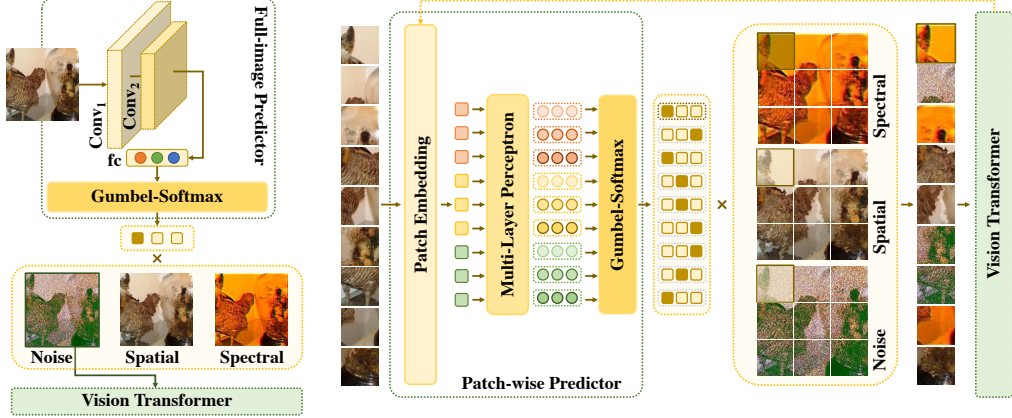


Figure 2: The outline of dynamic augmentation predictor. The full-image predictor lies in left side and it output a prediction for each instance. Patch-wise predictor situates on right side and each patch will match with individual decision. Decisions acquired by predictor will be multiplied with augmented image or patches before sent into ViT.

ment of input-conditional parameters. Not only that, spectral filter is better in Fog and diffeomorphism is helpful for Elastic Transform (please refer to Appendix B). Despite that these two augmentations are inferior to conditional ANT in robustness, their stability towards clean accuracy is clearly shown.

4.3 Dynamic Augmentation Selection

Random sampling and mixing strategies are crucial for data augmentations [18, 31, 57]. However, there still lacks study in input-based augmentation policies. Moreover, notably in section 4.2, conditional ANT is inferior in clean recognition in spite of advantage in robustness while conditional spectral filter and diffeomorphism are the opposite. Considering the trade-off, we wish to incorporate these complementary augmentations in a most appropriate way. Therefore, we introduce a dynamic augmentation selection approach and show that it achieves the best trade-off between clean accuracy and robustness.

Dynamic predictor We select augmentations in two different manners: (1) Predicting one proper augmentation for each full image; (2) Predicting one suitable perturbation for each patch. See Fig. 2 for an overview.

For **full-image prediction**, we use a CNN-based structures as a predictor to choose an augmentation conditioned on inputs. In particular, an input-sample x will be fed into two convolution layers,

$$\begin{aligned} f^1 &= \text{MaxPool}(\text{ReLU}(\text{BN}_1(\text{Conv}_1(x)))), \\ f^2 &= \text{Dropout}(\text{AvgPool}(\text{ReLU}(\text{BN}_2(\text{Conv}_2(f^1))))). \end{aligned} \quad (10)$$

Consequently, probabilities $p^1 \in \mathbb{R}^m$ of m augmentations $\{\mathcal{P}_1, \dots, \mathcal{P}_m\}$ are generated by projecting f^2 into a fully-connected layer. To find the augmentation with maximal score, non-differentiable Top-1 selection should be made feasible for end-to-end training. We further process the output with Gumbel-Softmax [23] to produce one-hot hard decision $h^1 = \{0, 1\}^m$ (details is presented in Appendix A.3). Meanwhile, we prepare images cast with different perturbations, which can be denoted as $\tilde{X} = \{\mathcal{P}_1(x), \dots, \mathcal{P}_m(x)\}$. Finally, the augmented image can be obtained by readily summing $h^1 \cdot \tilde{X}$ up.

For **patch-wise predictor**, we first turn $x \in \mathbb{R}^{C \times H \times W}$ into tokens $t \in \mathbb{R}^{T \times D}$ by reusing learned patch embedding layer of ViT, where T refers to number of tokens. To acquire scores of different patches, we employ following Multi-Layer Perceptron (MLP) layers,

Table 11: Results of dynamic augmentation selection on pre-trained DeiT-S. Experiments are conducted with smaller perturbation learning rate of $2e^{-5}$ (Please refer to single augmentation results under lr of $2e^{-5}$ in Table 15). Words in Method column refer to the unit of selection.

Augmentation	Method	Decision	Entropy	IN Acc↑	IN-C Acc↑	IN-C mCE↓
ANT 1x1 + SF. 3x3 + Diffeo.	element	Hard	×	81.01	61.84	48.97
ANT 1x1 + SF. 3x3 + Diffeo.	patch	Hard	×	80.87	60.01	51.24
ANT 1x1 + SF. 3x3 + Diffeo.	element	Soft	×	80.96	61.73	49.15
ANT 1x1 + SF. 3x3 + Diffeo.	element	Soft	✓	80.76	62.02	48.79

$$\begin{aligned} f^1 &= [\text{M1p}_1(t), \text{AvgPool}(\text{M1p}_1(t))], \\ f^2 &= \text{M1p}_2(f^1). \end{aligned} \quad (11)$$

Afterwards, probabilities $p^2 \in \mathbb{R}^{T \times m}$ are computed by applying Softmax to f^2 . Similarly, Gumbel-Softmax trick is implemented to get final hard decision $h^2 = \{0, 1\}^{T \times m}$. Therefore, token t_i is finally transformed to

$$\hat{t}_i = \sum_{j=0}^m h_{i,j}^2 \cdot P_j(t_i). \quad (12)$$

Trade-off between clean and corrupted data We train the predictor collaboratively with ViT in defense phase. To avoid the predictor from badly inclining to either strongest augmentations or harmless ones, we introduce an entropy term [30, 48] that are widely used in reinforcement learning to encourage better exploration,

$$L_{\text{entropy}} = -\mu \cdot \left(-\sum_i \hat{h}_i \log \hat{h}_i \right), \quad (13)$$

where \hat{h}_i denotes soft decisions generated by Gumbel-Softmax and μ is set to 0.5 in experiments. Without maximum-entropy penalty, we re-initialize predictor in each epoch to guarantee diversity.

The experimental results in Table 11 reflect an evident trade-off between accuracy on clean and corrupted data. While predictors experience a slight drop in robustness, they are much more superior in maintaining accuracy on clean data. Moreover, patch-varied augmentations lead to worse results, which might be ascribed to the mismatch between training and testing distribution, since actual inputs share same pattern in all patches. However, it implies that ViTs still fail in encoding inputs varying in distribution to unified semantic feature.

5 Conclusion

In this work, we provided deeper insights into ViTs’ robustness towards common corruptions by walking through impact of CNN-like backbone design choices and transferability of CNN-based methods to ViTs. We also proposed novel conditional augmentation strategy consists of two techniques. With first one utilizing instance-dependent augmentation parameters to improve robustness, the second means predicted an ideal category of augmentations and improved performance on clean data. Comprehensive experiments were conducted and thorough investigations were delivered above.

References

- [1] Yutong Bai, Jieru Mei, Alan L Yuille, and Cihang Xie. Are transformers more robust than cnns? In *NeurIPS*, 2021.
- [2] Srinadh Bhojanapalli, Ayan Chakrabarti, Daniel Glasner, Daliang Li, Thomas Unterthiner, and Andreas Veit. Understanding robustness of transformers for image classification. In *ICCV*, 2021.
- [3] Chun-Fu Chen, Rameswar Panda, and Quanfu Fan. Regionvit: Regional-to-local attention for vision transformers. In *ICLR*, 2022.
- [4] Chun-Fu Richard Chen, Quanfu Fan, and Rameswar Panda. Crossvit: Cross-attention multi-scale vision transformer for image classification. In *ICCV*, 2021.
- [5] Guangyao Chen, Peixi Peng, Li Ma, Jia Li, Lin Du, and Yonghong Tian. Amplitude-phase recombination: Rethinking robustness of convolutional neural networks in frequency domain. In *ICCV*, 2021.
- [6] Yinpeng Chen, Xiyang Dai, Mengchen Liu, Dongdong Chen, Lu Yuan, and Zicheng Liu. Dynamic convolution: Attention over convolution kernels. In *CVPR*, 2020.
- [7] François Chollet. Xception: Deep learning with depthwise separable convolutions. In *CVPR*, 2017.
- [8] Xiangxiang Chu, Zhi Tian, Yuqing Wang, Bo Zhang, Haibing Ren, Xiaolin Wei, Huaxia Xia, and Chunhua Shen. Twins: Revisiting the design of spatial attention in vision transformers. In *NeurIPS*, 2021.
- [9] Ekin D Cubuk, Barret Zoph, Dandelion Mane, Vijay Vasudevan, and Quoc V Le. Autoaugment: Learning augmentation policies from data. In *CVPR*, 2019.
- [10] Ekin D Cubuk, Barret Zoph, Jonathon Shlens, and Quoc V Le. Randaugment: Practical automated data augmentation with a reduced search space. In *CVPR Workshops*, 2020.
- [11] Alexey Dosovitskiy, Lucas Beyer, Alexander Kolesnikov, Dirk Weissenborn, Xiaohua Zhai, Thomas Unterthiner, Mostafa Dehghani, Matthias Minderer, Georg Heigold, Sylvain Gelly, Jakob Uszkoreit, and Neil Houlsby. An image is worth 16x16 words: Transformers for image recognition at scale. In *ICLR*, 2021.
- [12] Songwei Ge, Shlok Mishra, Chun-Liang Li, Haohan Wang, and David Jacobs. Robust contrastive learning using negative samples with diminished semantics. In *NeurIPS*, 2021.
- [13] Yizeng Han, Gao Huang, Shiji Song, Le Yang, Honghui Wang, and Yulin Wang. Dynamic neural networks: A survey. *IEEE TPAMI*, 2021.
- [14] Ali Hassani, Steven Walton, Nikhil Shah, Abulikemu Abuduweili, Jiachen Li, and Humphrey Shi. Escaping the big data paradigm with compact transformers. *arXiv preprint arXiv:2104.05704*, 2021.
- [15] Kaiming He, Xinlei Chen, Saining Xie, Yanghao Li, Piotr Dollár, and Ross Girshick. Masked autoencoders are scalable vision learners. *arXiv preprint arXiv:2111.06377*, 2021.
- [16] Dan Hendrycks, Steven Basart, Norman Mu, Saurav Kadavath, Frank Wang, Evan Dorundo, Rahul Desai, Tyler Zhu, Samyak Parajuli, Mike Guo, et al. The many faces of robustness: A critical analysis of out-of-distribution generalization. In *ICCV*, 2021.
- [17] Dan Hendrycks and Thomas Dietterich. Benchmarking neural network robustness to common corruptions and perturbations. In *ICLR*, 2018.
- [18] Dan Hendrycks, Norman Mu, Ekin D Cubuk, Barret Zoph, Justin Gilmer, and Balaji Lakshminarayanan. Augmix: A simple data processing method to improve robustness and uncertainty. In *ICLR*, 2019.
- [19] Dan Hendrycks, Norman Mu, Ekin D Cubuk, Barret Zoph, Justin Gilmer, and Balaji Lakshminarayanan. Augmix: A simple data processing method to improve robustness and uncertainty. In *ICLR*, 2020.
- [20] Dan Hendrycks, Andy Zou, Mantas Mazeika, Leonard Tang, Dawn Song, and Jacob Steinhardt. Pixmix: Dreamlike pictures comprehensively improve safety measures. In *NeurIPS*, 2021.
- [21] Byeongho Heo, Sangdoo Yun, Dongyoon Han, Sanghyuk Chun, Junsuk Choe, and Seong Joon Oh. Rethinking spatial dimensions of vision transformers. In *ICCV*, 2021.

[22] Charles Herrmann, Kyle Sargent, Lu Jiang, Ramin Zabih, Huiwen Chang, Ce Liu, Dilip Krishnan, and Deqing Sun. Pyramid adversarial training improves vit performance. *arXiv preprint arXiv:2111.15121*, 2021.

[23] Eric Jang, Shixiang Gu, and Ben Poole. Categorical reparameterization with gumbel-softmax. In *ICLR*, 2017.

[24] Boyi Li, Felix Wu, Ser-Nam Lim, Serge Belongie, and Kilian Q. Weinberger. On feature normalization and data augmentation. In *CVPR*, 2021.

[25] Ze Liu, Yutong Lin, Yue Cao, Han Hu, Yixuan Wei, Zheng Zhang, Stephen Lin, and Baining Guo. Swin transformer: Hierarchical vision transformer using shifted windows. In *ICCV*, 2021.

[26] Ilya Loshchilov and Frank Hutter. Decoupled weight decay regularization. In *ICLR*, 2018.

[27] Kaleel Mahmood, Rigel Mahmood, and Marten van Dijk. On the robustness of vision transformers to adversarial examples. In *ICCV*, 2021.

[28] Chengzhi Mao, Lu Jiang, Mostafa Dehghani, Carl Vondrick, Rahul Sukthankar, and Irfan Essa. Discrete representations strengthen vision transformer robustness. In *ICLR*, 2022.

[29] Xiaofeng Mao, Gege Qi, Yuefeng Chen, Xiaodan Li, Ranjie Duan, Shaokai Ye, Yuan He, and Hui Xue. Towards robust vision transformer. *arXiv preprint arXiv:2105.07926*, 2021.

[30] Volodymyr Mnih, Adria Puigdomenech Badia, Mehdi Mirza, Alex Graves, Timothy Lillicrap, Tim Harley, David Silver, and Koray Kavukcuoglu. Asynchronous methods for deep reinforcement learning. In *ICML*, 2016.

[31] Apostolos Modas, Rahul Rade, Guillermo Ortiz-Jiménez, Seyed-Mohsen Moosavi-Dezfooli, and Pascal Frossard. Prime: A few primitives can boost robustness to common corruptions. *arXiv preprint arXiv:2112.13547*, 2021.

[32] Muhammad Muzammal Naseer, Kanchana Ranasinghe, Salman H Khan, Munawar Hayat, Fahad Shahbaz Khan, and Ming-Hsuan Yang. Intriguing properties of vision transformers. In *NeurIPS*, 2021.

[33] Sayak Paul and Pin-Yu Chen. Vision transformers are robust learners. In *AAAI*, 2022.

[34] Leonardo Petrini, Alessandro Favero, Mario Geiger, and Matthieu Wyart. Relative stability toward diffeomorphisms indicates performance in deep nets. In *NeurIPS*, 2021.

[35] Yongming Rao, Wenliang Zhao, Benlin Liu, Jiwen Lu, Jie Zhou, and Cho-Jui Hsieh. Dynamiccvit: Efficient vision transformers with dynamic token sparsification. In *NeurIPS*, 2021.

[36] Evgenia Rusak, Lukas Schott, Roland S Zimmermann, Julian Bitterwolf, Oliver Bringmann, Matthias Bethge, and Wieland Brendel. A simple way to make neural networks robust against diverse image corruptions. In *ECCV*, 2020.

[37] Vivek Sharma, Ali Diba, Davy Neven, Michael S Brown, Luc Van Gool, and Rainer Stiefelhagen. Classification-driven dynamic image enhancement. In *CVPR*, 2018.

[38] Manli Shu, Yu Shen, Ming C. Lin, and Tom Goldstein. Adversarial differentiable data augmentation for autonomous systems. In *ICRA*, 2021.

[39] Manli Shu, Zuxuan Wu, Micah Goldblum, and Tom Goldstein. Encoding robustness to image style via adversarial feature perturbations. In *NeurIPS*, 2021.

[40] Teppei Suzuki. Teachaugment: Data augmentation optimization using teacher knowledge. In *CVPR*, 2022.

[41] Hugo Touvron, Matthieu Cord, Matthijs Douze, Francisco Massa, Alexandre Sablayrolles, and Hervé Jégou. Training data-efficient image transformers & distillation through attention. In *ICML*, 2021.

[42] Haotao Wang, Chaowei Xiao, Jean Kossaifi, Zhiding Yu, Anima Anandkumar, and Zhangyang Wang. Augmax: Adversarial composition of random augmentations for robust training. In *NeurIPS*, 2021.

[43] Wenhui Wang, Enze Xie, Xiang Li, Deng-Ping Fan, Kaitao Song, Ding Liang, Tong Lu, Ping Luo, and Ling Shao. Pyramid vision transformer: A versatile backbone for dense prediction without convolutions. In *ICCV*, 2021.

[44] Wenhui Wang, Enze Xie, Xiang Li, Deng-Ping Fan, Kaitao Song, Ding Liang, Tong Lu, Ping Luo, and Ling Shao. Pvttv2: Improved baselines with pyramid vision transformer. *CVMJ*, 2022.

[45] Wenxiao Wang, Lu Yao, Long Chen, Binbin Lin, Deng Cai, Xiaofei He, and Wei Liu. Crossformer: A versatile vision transformer hinging on cross-scale attention. In *ICLR*, 2022.

[46] Ross Wightman. Pytorch image models. <https://github.com/rwightman/pytorch-image-models>, 2019.

[47] Haiping Wu, Bin Xiao, Noel Codella, Mengchen Liu, Xiyang Dai, Lu Yuan, and Lei Zhang. Cvt: Introducing convolutions to vision transformers. In *ICCV*, 2021.

[48] Yuxin Wu and Yuandong Tian. Training agent for first-person shooter game with actor-critic curriculum learning. In *ICLR*, 2017.

[49] Cihang Xie, Mingxing Tan, Boqing Gong, Jiang Wang, Alan L Yuille, and Quoc V Le. Adversarial examples improve image recognition. In *CVPR*, 2020.

[50] Zhenda Xie, Zheng Zhang, Yue Cao, Yutong Lin, Jianmin Bao, Zhuliang Yao, Qi Dai, and Han Hu. Simmim: A simple framework for masked image modeling. *arXiv preprint arXiv:2111.09886*, 2021.

[51] Qinwei Xu, Ruipeng Zhang, Ya Zhang, Yanfeng Wang, and Qi Tian. A fourier-based framework for domain generalization. In *CVPR*, 2021.

[52] Brandon Yang, Gabriel Bender, Quoc V Le, and Jiquan Ngiam. Condconv: Conditionally parameterized convolutions for efficient inference. In *NeurIPS*, 2019.

[53] Dong Yin, Raphael Gontijo Lopes, Jon Shlens, Ekin Dogus Cubuk, and Justin Gilmer. A fourier perspective on model robustness in computer vision. In *NeurIPS*, 2019.

[54] Kun Yuan, Shaopeng Guo, Ziwei Liu, Aojun Zhou, Fengwei Yu, and Wei Wu. Incorporating convolution designs into visual transformers. In *ICCV*, 2021.

[55] Li Yuan, Yunpeng Chen, Tao Wang, Weihao Yu, Yujun Shi, Zi-Hang Jiang, Francis EH Tay, Jiashi Feng, and Shuicheng Yan. Tokens-to-token vit: Training vision transformers from scratch on imagenet. In *ICCV*, 2021.

[56] Sangdoo Yun, Dongyoon Han, Seong Joon Oh, Sanghyuk Chun, Junsuk Choe, and Youngjoon Yoo. Cutmix: Regularization strategy to train strong classifiers with localizable features. In *ICCV*, 2019.

[57] Hongyi Zhang, Moustapha Cisse, Yann N Dauphin, and David Lopez-Paz. mixup: Beyond empirical risk minimization. In *ICLR*, 2018.

[58] Xinyu Zhang, Qiang Wang, Jian Zhang, and Zhao Zhong. Adversarial autoaugment. In *ICLR*, 2019.

[59] Yikang Zhang, Jian Zhang, Qiang Wang, and Zhao Zhong. Dynet: Dynamic convolution for accelerating convolutional neural networks. *arXiv preprint arXiv:2004.10694*, 2020.

[60] Zizhao Zhang, Han Zhang, Long Zhao, Ting Chen, and Tomas Pfister. Aggregating nested transformers. In *AAAI*, 2022.

[61] Mingjian Zhu, Kai Han, Enhua Wu, Qiulin Zhang, Ying Nie, Zhenzhong Lan, and Yunhe Wang. Dynamic resolution network. In *NeurIPS*, 2021.

Appendix

A An Overall Robustness Evaluation

Model	Hierarchical	#Param(M)	IN		IN-C
			Acc↑	Acc↑	mCE↓
T2T-ViT-7 [55]	✗	4.3	71.49	39.45	77.02
PiT-T [21]	✓	4.9	72.84	45.70	69.11
ViT-T [11]	✗	5.7	75.49	42.64	72.50
DeiT-T [41]	✗	5.7	72.14	44.23	71.13
CrossViT-T [4]	✗	7.0	73.35	45.70	69.35
PVTv1-T [43]	✓	13.2	75.00	37.94	79.56
RegionViT-T [3]	✓	13.8	80.13	53.99	58.74
PVTv2-B1 [44]	✓	14.0	78.70	50.81	62.65
NesT-T [60]	✓	17.1	81.37	55.93	56.39
CvT-13 [47]	✓	20.0	81.62	55.27	57.06
T2T-ViT-14 [55]	✗	21.5	81.38	57.91	53.59
DeiT-S [41]	✗	22.0	79.83	57.20	54.60
ViT-S [11]	✗	22.1	81.40	58.31	52.95
PiT-S [21]	✓	23.5	80.98	58.88	52.47
Twins-PCPVT-S [8]	✓	24.1	81.21	56.31	55.85
PVTv1-S [43]	✓	24.5	79.79	47.89	66.89
PVTv2-B2 [44]	✓	25.4	82.02	58.92	52.56
CrossViT-S [4]	✗	26.9	80.97	59.23	52.03
CrossFormer-T [45]	✓	27.8	81.51	57.48	54.39
Swin-T [25]	✓	28.3	81.16	51.59	61.96
RegionViT-S [3]	✓	30.6	82.60	58.86	52.62
CrossFormer-S [45]	✓	30.7	82.45	58.47	53.19
CvT-21 [47]	✓	31.6	82.46	58.04	53.52
NesT-S [60]	✓	38.3	83.04	60.22	50.83
T2T-ViT-19 [55]	✗	39.1	81.70	59.38	51.75
RegionViT-M [3]	✓	41.2	83.08	60.41	50.67
Twins-PCPVT-B [8]	✓	43.8	82.74	59.64	51.63
PVTv1-M [43]	✓	44.2	81.31	51.34	62.39
Swin-S [25]	✓	49.6	83.17	57.16	54.92
CrossFormer-B [45]	✓	52.0	83.43	61.66	49.10
Twins-PCPVT-L [8]	✓	61.0	83.05	60.03	51.13
PVTv1-L [43]	✓	61.4	81.72	53.33	59.86
T2T-ViT-24 [55]	✗	64.0	82.06	61.44	49.10
NesT-B [60]	✓	67.7	83.62	61.10	49.84
RegionViT-B [3]	✓	72.7	83.16	60.02	51.18
PiT-B [21]	✓	73.8	82.39	62.39	48.16
PVTv2-B5 [44]	✓	82.0	83.77	64.12	45.90
DeiT-B [41]	✗	86.6	81.80	62.06	48.52
Ours	✗	86.6	82.35	68.38	40.68
Swin-B [25]	✓	88.0	83.75	57.51	66.70
CrossViT-B [4]	✗	105.0	82.14	63.25	46.92

Table 12: A thorough analysis of ViTs robustness. Models’ weights are all acquired from official public resources except for ViT’s weights, which are provided by timm [46]. **Ours** indicates fine-tuned DeiT-B on conditional adversarial speckle noise.

Here (Table 12) we display a complete version of Table 1. We conduct a thorough evaluation on robustness benchmarking datasets ImageNet-C [17] of existing Vision Transformers (*i.e.* ViT [11], DeiT [41], Token-to-Token ViT [55], Cross ViT [4], PiT [21], CvT [47], Twins-PCPVT [8], RegionViT [3], CrossFormer [45], NesT [60], PVT [43, 44] and Swin Transformer [25]). The listed models are all trained on ImageNet-1k data and sorted by Parameters in ascending order. Among hierarchical ViTs, PVTv1s and Swin Transformers have inferior resistance towards common corruptions while others achieve similar performance with non-hierarchical backbones. Especially, PVTv2s shows an

obvious advantage over robustness. We also append measure of our conditional method on DeiT-B, notably, it beats all existing models by a large margin.

Regarding input resolution of 224×224 , images in most datasets are in higher resolution and not uniform in size. Usually, samples should first be rescaled to 256 and cropped to a central area of 224×224 before fed into networks. However, it's noteworthy that samples in ImageNet-C have already been preprocessed to shape of 224×224 . Hence, to ensure a rigorous evaluation, usual resizing operation will result in up-sampling on ImageNet-C and should be removed.

A.1 Enhance Robustness of Swin Transformer

Table 13: Results of Swin-T replaced with different designs in Feed-Forward Network and Patch Embedding. Here we set k to 4 for conditional DWConv.

Model	#Params (M)	IN Acc \uparrow	IN-C Acc \uparrow	IN-C mCE \downarrow
Swin-T	28.29	81.16	51.59	61.96
+ DWConv in FFN	28.46	81.83	56.73	55.28
+ Cond. DWConv in FFN	28.84	81.95	56.69	55.34
+ Overlapping PE. 18×18	28.29	81.61	54.75	57.74
+ Overlapping PE. 20×20	28.30	81.59	54.96	57.54
+ Overlapping PE. 24×24	28.33	81.52	56.11	56.11

In main paper, it is verified that overlapping patch embedding (Overlapping PE) and convolution Feed-forward Network (FFN) can facilitate robustness on non-hierarchical ViT (DeiT). To further explore their effectiveness, we adapt these two designs for Swin-T. As shown in Table 13, they contribute to a marked rise in performance once again. Different from results on DeiT-S, patch embeddings with larger kernel size bring about more advantage on robustness performance.

A.2 Ablation Studies for Conditional Augmentation

Here we display extended ablation study on adversarial noise training (ANT) and dynamic augmentation selection.

As Table 14 displays, observably, dynamic parameters can boost ANT's performance towards common corruptions on PiT-S and ViT-S as well. Despite that adversarial Speckle noise is slightly inferior to Gaussian noise on PiT-S and ViT-S, our method manages to fulfil Speckle noise's potential by surpassing its counterpart with conditional strategy. In Table 15, we demonstrate results of dynamic augmentations on pre-trained DeiT-S and PiT-S. Distinguished from results attached in main paper, experiments in Table 15 incorporate augmentations with conditional parameters while still demonstrate most favorable trade-off between performance on clean and corrupted data.

Method	Pre-trained	Norm	IN	IN-C		IN-C w/o Noise Acc \uparrow
			Acc \uparrow	Acc \uparrow	mCE \downarrow	
PiT-S [21]	\times	-	80.98	58.88	52.47	58.38
+ ANT Gaussian 1×1	\checkmark	80	80.77	62.86	47.60	61.09
+ Cond ANT Gaussian 1×1	\checkmark	80	80.80	63.13	47.28	61.52
+ ANT Speckle 1×1	\checkmark	80	80.93	62.77	47.71	60.98
+ Cond ANT Speckle 1×1	\checkmark	80	80.74	63.64	46.63	62.05
ViT-S [11]	\times	-	80.37	57.69	53.99	57.40
+ ANT Gaussian 1×1	\checkmark	80	80.49	62.60	47.95	60.80
+ ANT Cond Gaussian 1×1	\checkmark	80	80.43	62.80	47.75	60.89
+ ANT Speckle 1×1	\checkmark	80	80.59	62.04	48.65	60.27
+ Cond ANT Speckle 1×1	\checkmark	80	80.60	64.08	46.18	61.95

Table 14: Ablation Study of ANT on pre-trained PiT-S and ViT-S.

Table 15: Ablation Study of pre-trained DeiT-S and PiT-S with dynamic augmentation selected by full-image predictor with learning rate set to $2e^{-5}$. The applied augmentation is implemented with conditional parameters.

Method	Decision	Entropy	IN	IN-C	
			Acc↑	Acc↑	mCE↓
DeiT-S + ANT 1x1	-	-	80.34	62.24	48.42
DeiT-S + SF. 3x3	-	-	81.15	60.22	50.92
DeiT-S + Diffeo.	-	-	81.00	61.25	49.50
DeiT-S + Cond ANT Speckle 1x1 + SF. 3x3 + Diffeo.	Hard	✗	80.81	62.97	47.42
DeiT-S + Cond ANT Speckle 1x1 + SF. 3x3 + Diffeo.	Hard	✓	80.89	62.73	47.73
DeiT-S + Cond ANT Speckle 1x1 + SF. 3x3 + Diffeo.	Soft	✗	80.88	62.42	48.15
DeiT-S + Cond ANT Speckle 1x1 + SF. 3x3 + Diffeo.	Soft	✓	80.77	62.39	48.19
PiT-S + Cond ANT Speckle 1x1 + SF. 3x3 + Diffeo.	Hard	✗	81.16	63.80	46.29
PiT-S + Cond ANT Speckle 1x1 + SF. 3x3 + Diffeo.	Hard	✓	81.15	64.02	46.00
PiT-S + Cond ANT Speckle 1x1 + SF. 3x3 + Diffeo.	Soft	✗	81.16	63.36	46.84
PiT-S + Cond ANT Speckle 1x1 + SF. 3x3 + Diffeo.	Soft	✓	81.14	63.02	47.25

A.3 Gumbel-Softmax in Augmentation Selection

In this section, we present a detailed procedure of how prediction is turned into differentiable decision by Gumbel-Softmax [23].

For prediction $p \in \mathbb{R}^m$ for a single image or patch, we first convert it into variable $d \in \mathbb{R}^m$ obeying Gumbel distribution, which models the distribution of maximum value,

$$d_i = \log(p_i) + G_i, \quad G_i \sim -\log(-\log(\text{Uniform}(0, 1))). \quad (14)$$

To obtain one-hot decision while getting around undifferentiable argmax operation, softmax is introduced with temperature τ ,

$$h_i = \frac{\exp((\log(p_i) + G_i)/\tau)}{\sum_{j=1}^k \exp((\log(p_j) + G_j)/\tau)}, \quad (15)$$

where h approaches one-hot vector when $\tau \rightarrow 0$. In implementation, τ is set to 1 to get a soft decision. For hard decision, we proceed by discretizing directly to get one-hot output whereas keeping the according soft decision for gradient computation.

Table 16: Results of DeiT-S with different experimental settings. OPE stands for overlapping patch embedding and FFN_{conv} refers to FFN injected with DWConv, while conv* indicates conditional DWConv. ‡ suggests training is conducted in fine-tuning manner. Diffeo., SF. and Speckle. are abbreviated forms for conditional agumentation of diffeomorphism, spectral filter and speckle noise respectively.

Method	Gauss.	Noise Impulse	Shot	Weather			Defoc.	Blur	Digital			mCE
				Bright.	Fog	Frost	Snow		Glass	Motion	Zoom	
DeiT-S	46.91	46.78	48.42	45.21	46.32	47.16	51.16	61.87	71.36	58.40	71.70	42.99
+ OPE _{k=1}	43.60	43.60	44.53	43.31	43.27	46.16	48.72	59.65	71.25	56.86	69.20	40.40
+ OPE _{k=2}	44.19	44.03	45.36	43.63	46.01	45.34	49.33	60.71	71.37	57.88	71.50	40.25
+ OPE _{k=4}	43.98	43.74	45.00	44.28	43.18	45.47	50.67	60.92	71.43	56.39	71.41	40.91
+ FFN _{conv}	44.60	44.52	45.35	43.59	45.17	46.34	47.84	59.39	70.06	54.25	69.37	40.97
+ FFN _{conv*}	45.40	45.60	45.77	44.97	44.61	47.27	49.10	60.07	71.22	56.19	69.36	40.04
DeiT-S ‡	43.85	43.52	46.26	42.69	42.16	44.81	48.85	59.23	69.55	56.50	69.78	39.31
+ Diffeo.	37.81	37.41	38.60	43.65	43.65	44.76	49.43	59.97	58.54	56.82	65.04	39.33
+ SF.	38.46	38.64	39.28	41.85	41.39	43.25	47.78	59.96	72.01	56.83	71.53	36.40
+ Speckle.	31.10	30.57	30.56	41.91	48.51	40.24	45.09	54.60	60.65	54.38	65.51	39.51

B Robustness towards Specific Corruption

As illustrated in Table 16 and Figure 4, DeiT-S with overlapping embedding outperforms in corruptions of Noise, Brightness, JPEG Compression, Contrast and Pixelation. Also, convolutional designs boost accuracy on corruptions from similar categories.



Figure 3: Visualizing 3 types of augmentations generated by our conditional adversarial method in different epochs. The top row refers to augmentations in spectral domain, images in middle row refer to noise perturbations and the bottom row exhibits samples augmented in spatial domain.

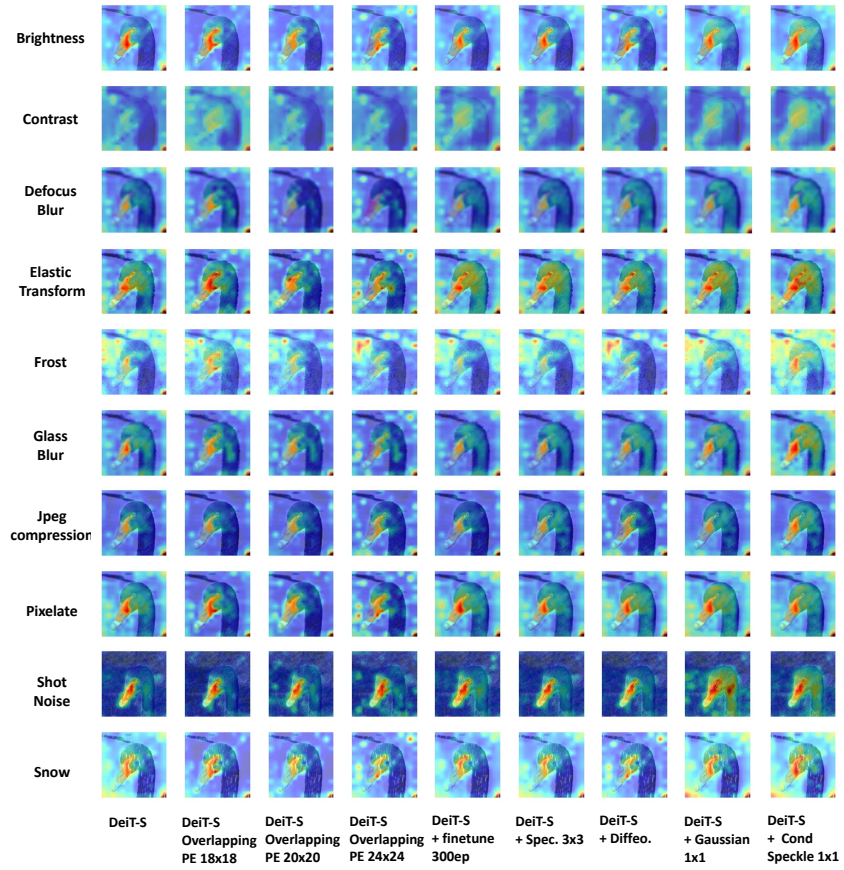


Figure 4: Visualizing attention in DeiT-S towards input samples cast with different corruptions.

Moreover, augmentations in spectral, spatial and domains are complementary to noise adversarial training. Since diffeomorphism brings better resilience towards Glass Blur and Elastic Transform, spectral transformation leads to stronger robustness against Contrast, Brightness and Fog.